Nature of the Inhibition of Horseradish Peroxidase and Mitochondrial Cytochrome *c* Oxidase by Cyanyl Radical

Yeong-Renn Chen,*,‡ Leesa J. Deterding,§ Kenneth B. Tomer,§ and Ronald P. Mason‡

Laboratories of Pharmacology and Chemistry and of Structural Biology, National Institute of Environmental Health Sciences, National Institutes of Health, Research Triangle Park, North Carolina 27709

Received November 16, 1999; Revised Manuscript Received February 1, 2000

ABSTRACT: Previous studies established that the cyanyl radical (•CN), detected as 5,5-dimethyl-1-pyrroline *N*-oxide (DMPO)/•CN by the electron spin resonance (ESR) spin-trapping technique, can be generated by horseradish peroxidase (HRP) in the presence of hydrogen peroxide (H_2O_2) and by mitochondrial cytochrome *c* oxidase (CcO) in the absence of H_2O_2. To investigate the mechanism of inhibition by cyanyl radical, we isolated and characterized the iron protoporphyrin IX and heme *a* from the reactions of CN^- with HRP and CcO, respectively. The purified heme from the reaction mixture of HRP/H_2O_2/KCN was unambiguously identified as cyanoheme by the observation of the protonated molecule, $(M + H)^+$, of $m/z = 642.9$ in the matrix-assisted laser desorption/ionization (MALDI) mass spectrum. The proton NMR spectrum of the bipyridyl ferrous cyanoheme complex revealed that one of the four *meso* protons was missing and had been replaced with a cyanyl group, indicating that the single, heme-derived product was *meso*-cyanoheme. The holoenzyme of HRP from the reconstitution of *meso*-cyanoheme with the apoenzyme of HRP (apoHRP) showed no detectable catalytic activity. The Soret peak of cyanoheme-reconstituted apoHRP was shifted to 411 nm from the 403 nm peak of native HRP. In contrast, the heme *a* isolated from partially or fully inhibited CcO did not show any change in the structure of the protoporphyrin IX as indicated by its MALDI mass spectrum, which showed an $(M + H)^+$ of $m/z = 853.6$, and by its pyridine hemochromogen spectrum. However, a protein-centered radical on the CcO can be detected in the reaction of CcO with cyanide and was identified as the thiyl radical(s) based on inhibition of its formation by *N*-ethylmaleimide pretreatment, suggesting that the protein matrix rather than protoporphyrin IX was attacked by the cyanyl radical. In addition to the difference in heme structures between HRP and CcO, the available crystallographic data also suggested that the distinct heme environments may contribute to the different inhibition mechanisms of HRP and CcO by cyanyl radical.

Cyanide has been widely used as an inhibitor to study hemoproteins, including many peroxidases and oxidases (*1*). In the case of a peroxidase such as horseradish peroxidase (HRP),[1] cyanide is able to replace the water in the sixth coordination position and inhibit its heme-catalyzed reactions. In the presence of hydrogen peroxide (H_2O_2), cyanide functions as a substrate for HRP compounds I and II and is oxidized to cyanyl radical (•CN), as detected by its 5,5-dimethyl-1-pyrroline *N*-oxide (DMPO)/•CN radical adduct (*2*). One-electron oxidation of cyanide to cyanyl radical (•CN) is also catalyzed by either chloroperoxidase or lactoperoxidase and, thus, is considered to be a general peroxidatic reaction (*2*, *3*).

In the case of mitochondrial cytochrome *c* oxidase (CcO), cyanide exhibits relatively high affinity to the dioxygen-binding site, the heme a_3-Cu_B binuclear center of the enzyme (*4*). The competition of cyanide with molecular oxygen for binding with the heme a_3-Cu_B binuclear center is typically thought to account for the inhibition of CcO by cyanide. In addition to serving as the ligand of heme a_3, cyanide also functions as the substrate for as-isolated CcO. A previous study established that the as-isolated CcO is capable of independently catalyzing the one-electron oxidation of cyanide to •CN (*5*). The small and variable amount of the catalytic intermediate compound P (related to HRP compound I) present in the enzyme preparation accounted for this reaction (*5*, *6*). It has been reported that the as-isolated CcO can carry out a peroxidase-like reaction at the heme a_3-Cu_B center with a high K_m for H_2O_2 (*7*, *8*). Therefore, in the presence of H_2O_2, the peroxidase activity of CcO oxidizes cyanide to •CN and presumably reduces compound P to compound F (related to HRP compound II) (*5*).

The enzymatic activity of either HRP or CcO is observed to be more vulnerable to cyanide in the presence of H_2O_2 than to cyanide alone, thus raising the questions, "Does a cyanyl radical contribute to the inhibition of enzyme activity?" and " What is the molecular mechanism of inhibition

* To whom correspondence should be addressed: Laboratory of Pharmacology and Chemistry, NIEHS, NIH, P.O. Box 12233, Research Triangle Park, NC 27709. Tel. 919-541-1501; Fax 919-541-1043; E-mail chen6@niehs.nih.gov.

‡ Laboratory of Pharmacology and Chemistry.

§ Laboratory of Structural Biology.

[1] Abbreviations: HRP, horseradish peroxidase; •CN, cyanyl radical; CcO, cytochrome *c* oxidase; DMPO, 5,5-dimethyl-1-pyrroline *N*-oxide; DTPA, diethylenetriaminepentaacetic acid; HPLC, high-performance liquid chromatography; MALDI, matrix-assisted laser desorption/ionization; apoHRP, apoenzyme of horseradish peroxidase; RT, retention time; NOE, nuclear Overhauser effect; •SCysCcO, cysteinyl thiyl radical; •OTyrCcO, tyrosyl radical.

10.1021/bi992652+
Published on Web 03/22/2000

of enzyme by the cyanyl radical?" To date, the fate and consequences of the cyanyl radical produced from either the HRP/H_2O_2/KCN or the CcO/KCN systems are unknown.

Recently, Eberson et al. (*9*, *10*) argued that trapping of the cyanyl radical might proceed via the so-called "inverted spin trapping phenomenon" (eq 1) in which the spin trap is oxidized to its radical cation, which then captures a nucleophile such as cyanide to give the radical adduct. It has also been argued that the formation of DMPO/•CN might proceed via the Forrester−Hepturn mechanism (eq 2), in which a hydroxylamine is formed by addition of a cyanide ion to the spin trap, which is air-oxidized to the adduct (*11*):

$$\text{DMPO} \xrightarrow{-e^-} \text{DMPO}^{\bullet +} \xrightarrow{CN^-} \text{DMPO/}^{\bullet}\text{CN} \quad (1)$$

$$\text{DMPO} + CN^- \xrightarrow{H^+} \text{DMPOH/CN} \xrightarrow{-e^-,\,-H^+} \text{DMPO/}^{\bullet}\text{CN} \quad (2)$$

The above arguments are supported only by thermodynamic calculations of a high oxidation potential for cyanide [$E°$-(•CN/CN^-) = 2.0 V] (*10*, *12*), which raises questions about the possibility of the enzyme-mediated generation of the cyanyl radical (*2*, *3*, *5*).

In this investigation, we report two different mechanism-based inhibitions by a cyanyl radical. In the HRP/H_2O_2/KCN system, the generated cyanyl radical reacts with the iron protoporphyrin IX of HRP. In the CcO/KCN system, the generated cyanyl radical reacts primarily with a cysteine residue(s) of the CcO protein matrix rather than with the CcO heme *a*. Our results are particularly important in three respects: (a) they support the existence of the cyanyl radical as detected by spin trapping (*9*, *10*), (b) they help to understand the relative roles of heme and protein in enzyme inhibition by cyanide; and (c) they provide relevance for the cyanyl radical to the oxidative damage induced by cyanide (*5*).

EXPERIMENTAL PROCEDURES

Reagents. Ascorbic acid, diethylenetriaminepentaacetic acid (DTPA), horseradish peroxidase type VI-A (EC 1.11.1.7), and guaiacol were purchased from Sigma Chemical Co. (St. Louis, MO) and used as received. Hydrogen peroxide was purchased from Fisher (St. Louis, MO). The H_2O_2 concentration was verified by its UV absorption at 240 nm (ϵ = 43.6 M^{-1} cm^{-1}). Potassium cyanide, pyridine-d_5, and tin(II) dichloride were purchased from Aldrich Chemical Co. (Milwaukee, WI). The 5,5-dimethyl-1-pyrroline *N*-oxide (DMPO) spin trap was purchased from Fluka Chemical Co. (St. Louis, MO), vacuum-distilled twice, and stored under liquid nitrogen at −70 °C until needed. The Sephadex G-25 column (PD-10) was purchased from Amersham Pharmacia Biotech (Piscataway, NJ). All reactions were performed in a 50 mM phosphate buffer (pH 7.4) treated with Chelex overnight. DTPA was added to a final concentration of 1 mM after treatment with Chelex.

Mitochondrial Cytochrome c Oxidase Preparation and Assay. Highly purified CcO was isolated from submitochondrial particles by the method developed by Yu et al. (*13*). Optical spectra were measured on an SLM Aminco DW-2000 UV/vis spectrophotometer (SLM Instruments, Inc.; Rochester, NY). The enzyme concentration (per aa_3) of CcO was calculated from the spectrum after dithionite reduction using an extinction coefficient of 24 $mM^{-1}cm^{-1}$ at 605 nm. The enzyme activity of CcO was assayed by measuring cytochrome *c* oxidation or oxygen consumption. An appropriate amount of CcO was added to an assay mixture (1 mL) containing 50 mM phosphate buffer, pH 7.4, and 60 μM reduced cytochrome *c*. The CcO activity was determined by measuring the decrease in absorbance at 550 nm. The oxygen consumption by CcO was measured as reported previously (*14*).

Analytical Methods. The concentration of HRP was determined by using an extinction coefficient of 102 mM^{-1} cm^{-1} at 402 nm. The enzyme activity was assayed by adding 5-μL aliquots of the reaction mixture to 1.0 mL of the assay mixture containing 3 mM guaiacol (2-methoxylphenol) and 0.5 mM H_2O_2 in 50 mM phosphate (pH 7.4) buffer, followed by measuring the increase in absorbance at 470 nm. High-performance liquid chromatography (HPLC) was performed on a Hewlett-Packard 1100 series HPLC system which was equipped with a vacuum degasser, a quaternary pump, and a diode array detector. ^{1}H NMR spectra were obtained on a Varian UnityPlus 500 MHz instrument in pyridine-d_5. Chemical shifts are reported in parts per million relative to tetramethylsilane. The analysis was done in the NIEHS/National Institutes of Health Laboratory of Structural Biology under the supervision of Dr. Robert E. London.

Electron Spin Resonance Experiments. Electron spin resonance (ESR) experiments were carried out on a Bruker ESP 300 ESR spectrometer operating at 9.8 GHz with 100 kHz modulation frequency at room temperature. The detailed procedure and instrumental parameters were the same as in the previous study (*5*). The spectral simulations were performed with the WinSim program of the NIEHS public ESR software package available over the Internet (*15*).

Mass Spectrometry. The mass spectrometric analyses were performed on a Voyager RP (Perseptive Biosystems, Framingham, MA) time-of-flight, dual-stage reflector mass spectrometer. The instrument uses a nitrogen laser at 337 nm to desorb/ionize the samples. The accelerating voltage used was 30 kV and the flight path was 1.3 m. A beam guide wire with an applied voltage was used to refocus dispersed ions back onto the detector. Data from up to 128 laser pulses were averaged on a Tektronix TDS 520A digitizing oscilloscope and then downloaded to a PC. Data analysis was performed with GRAMS 386 software. The MALDI matrix (0.5 μL of a saturated solution of α-cyano-4-hydroxycinnamic acid in 45:45:10 ethanol−water−formic acid) and 0.5 μL of an appropriate dilution of the samples were spotted onto the MALDI target. Cocrystallization of the sample and matrix was allowed to proceed at room temperature.

Isolation and Qualitative Analysis of the Hemes from the Cyanide-Inactivated HRP and Cyanide-Inactivated CcO. The iron protoporphyrin IX of cyanide-inactivated HRP was extracted into peroxide-free diethyl ether. The organic layer containing the heme was washed with NaCl-saturated water (once) and water (twice), dried over anhydrous sodium sulfate, and then evaporated to dryness under a stream of nitrogen. The residue was analyzed by reversed-phase HPLC on a Zorbax ODS column (4.6 × 250 mm) with 5-μm particles. The column was eluted at a flow rate of 1 mL/min with a linear gradient formed by solvents A and B, where solvent A is 65% ethanol containing 0.1% TFA and solvent B is 100% ethanol containing 0.1% TFA. The gradient rose

Table 1: Effect of KCN, H_2O_2 (A−E), and Heme Reconstitution (F−H) on HRP-Catalyzed Guaiacol Oxidation

experiments	preparations[a]	HRP activity (%)
A	HRP (50 μM)	100
B	HRP (50 μM) + KCN (2.5 mM)	95.2 ± 2.8
C	HRP (50 μM) + KCN (2.5 mM) + H_2O_2 (10 mM)	64.7 ± 2.0
D	HRP (50 μM) + KCN (5.0 mM) + H_2O_2 (10 mM)	52.8 ± 1.6
E	HRP (50 μM) + KCN (5.0 mM) + H_2O_2 (15 mM)	37.7 ± 1.1
F	apoHRP[b]	0
G	(apoHRP + heme)[b]	(95.0 ± 2.7)[c]
H	(apoHRP + *meso*-cyanoheme)[b]	0

[a] The reaction mixture containing HRP, KCN, and H_2O_2 in 200 μl of 50 mM phosphate buffer (pH 7.4) containing 1 mM DTPA was allowed to incubate at room temperature for 1 h. The mixture was passed through a Sephadex G-25 column and the fraction containing HRP was collected for measuring the enzymatic activity of guaiacol oxidation. [b] The methods of apoHRP preparation and heme reconstitution are described under "Experimental Procedures." [c] The enzyme activity here is calculated based on the heme concentration and normalized with that of native HRP.

from 0% to 50% solvent B over a period of 30 min, and the eluate was monitored at 402 nm.

The heme *a* from the cyanide-inactivated CcO was extracted and analyzed by the following procedure. Briefly, 1 mL of a mixture of CcO (200 μM) and potassium cyanide (10 mM) in 50 mM phosphate buffer, pH 7.4, containing 1 mM DTPA was incubated for 1 h at room temperature. The reaction mixture was mixed with 1 mL of cold acetone (−20 °C) containing 5% HCl (v/v). The mixture was allowed to stand on ice for 10 min with occasional vortexing. The mixture was then centrifuged at 250*g* for 5 min. The pellet was extracted with another 1 mL of cold acetone containing 5% HCl and then combined with the first supernatant. Two milliliters of diethyl ether were added to the acetone extract, and the mixture was washed with cold NaCl-saturated water and cold water to remove the acetone. The resulting organic layer containing heme *a* was recovered and dried under a stream of nitrogen. The purified heme *a* was determined by measuring the pyridine hemochromagen spectrum and analyzed by HPLC as described above.

Reconstitution of meso-Cyanoheme with the Apoenzyme of HRP. The Apoenzyme of HRP (apoHRP) was prepared by shaking 1 mL of HCl-acidified HRP (0.2 mM based on the heme) with three 1-ml aliquots of 2-butanone. More than 95% of the heme was removed, as judged by comparing the Soret absorbance at 402 nm between apoHRP and native HRP. *meso*-Cyanoheme, isolated from 30 mg of HRP, was dissolved in sodium borate buffer (pH 9.2) containing 1% KOH and added dropwise to the stirred apoHRP solution. The reconstituted enzyme was equilibrated with 50 mM phosphate buffer (pH 7.4) by gel filtration on a Sephadex G-25 column.

RESULTS

Irreversible Inhibition of HRP by Potassium Cyanide. To test whether the inhibition of HRP by cyanide in the HRP/H_2O_2/KCN system is irreversible or not, we incubated 1 equiv of HRP with 50 equiv of KCN and 200 equiv of H_2O_2 at room temperature for 1 h. The reaction mixture was subjected to gel filtration with Sephadex G-25 to remove excess cyanide and peroxide. The remaining enzyme activity of the eluting fraction containing HRP was then determined. As shown in Table 1, 35% inhibition of guaiacol oxidation was observed from this incubation (Table 1, experiment C). No significant change in HRP activity (less than 5%) was detected when H_2O_2 was omitted from the system (Table 1, experiment B). Further inhibition of the enzyme, however, required more KCN or H_2O_2 (Table 1, experiments D and E). The results indicate that the cyanyl radical functions as an irreversible inhibitor of HRP.

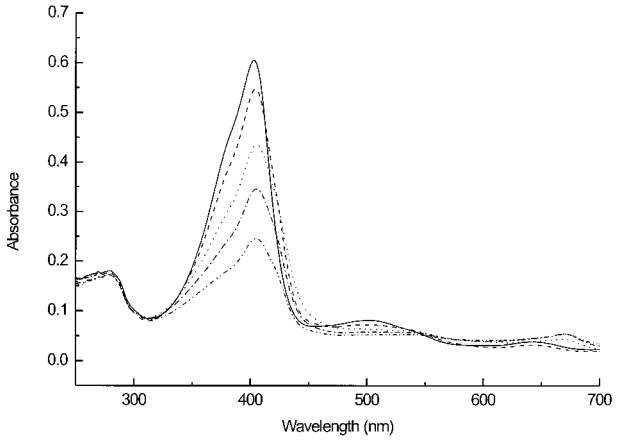

FIGURE 1: Spectroscopic changes accompanying the reaction of HRP (50 μM) with KCN (2.5 mM) in the presence of H_2O_2. The reaction conditions in the system were identical to those described in the legend of Table 1. The mixture was subjected to gel filtration at the end of incubation. The spectra show intact HRP (—), a mixture of HRP and KCN (- - -) with 10 mM H_2O_2 and 35% inhibition (•••), 20 mM H_2O_2 and 46% inhibition (- • -), and 40 mM H_2O_2 and 65% inhibition (- •• -).

Incubation of 50 μM HRP with 2.5 mM potassium cyanide (pH 7.4) at room temperature for 1 h caused an intensity decrease and a slight red shift in the Soret band (from λ_{max} = 402.9 nm to λ_{max} = 404.1 nm) after removal of excess cyanide by gel filtration (Figure 1). Replacement of the sixth ligand of HRP by cyanide accounted for this spectroscopic change. If the system contained H_2O_2, a further red shift and a further decrease in the intensity of the Soret band was observed, presumably due to the effect of the cyanyl radical (Figure 1). The intensity decrease parallels the amount of added H_2O_2 and the inhibition of enzyme activity as indicated in Figure 1. It was apparent that the additional spectral change was attributable to protoporphyrin IX modification. To address this additional effect, we isolated and characterized the heme from cyanide-inactivated HRP.

Isolation of Cyano-Derived Heme from Cyanide-Inactivated HRP. Incubation of 50 μM HRP and 5 mM KCN in the presence of 10 mM H_2O_2 (pH 7.4) at room temperature for 1 h gave roughly 47% inhibition of HRP. HPLC analysis (Figure 2) of the isolated heme products from the reaction mixture revealed an additional heme-derived product (cyano-derived heme) with a retention time (RT) of 4.6 min (Figure

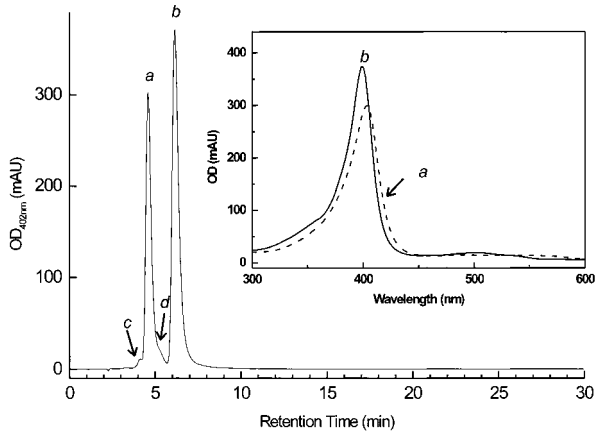

FIGURE 2: C_{18} reverse-phase HPLC chromatogram of heme residues extracted from the HRP/KCN reaction mixture in the presence of H_2O_2. The detailed conditions of HRP inhibition, heme isolation, and HPLC are described under Experimental Procedures. The eluting species a−d in the HPLC chromatogram are explained under Results. The Soret spectra collected with a diode array detector for the peaks at retention times of 4.6 min (dashed line, a) and 6.2 min (solid line, b) are shown in the inset.

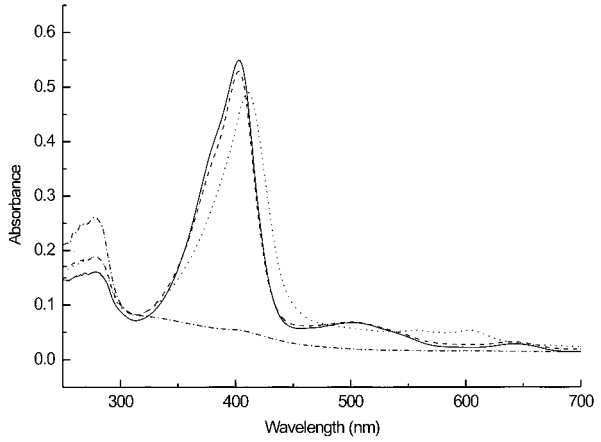

FIGURE 3: UV/vis absorption spectra of intact HRP, apoenzyme of HRP (apoHRP), heme-reconstituted apoHRP, and cyanoheme reconstituted apoHRP. The preparation of apoHRP from intact HRP and the conditions of heme reconstitution are described under Experimental Procedures. The sample was equilibrated with 50 mM phosphate buffer (pH 7.4) and passed through a Sephadex G-25 column before spectroscopic measurement. The spectra of intact HRP (—), heme-reconstituted apoHRP (- - -), cyanoheme-reconstituted apoHRP (···) and apoHRP (- · -) are shown.

2, peak a) in addition to the native heme group (RT = 6.2 min on the analytical column, Figure 2, peak b). The spectrum of the cyano-derived heme from the HPLC effluent as recorded by a diode array detector indicated that its Soret band shifts from 399 to 403 nm (Figure 2, inset).

Reconstitution of ApoHRP with Heme. As indicated in Figure 3, reconstitution of the cyano-derived heme with apoHRP yielded an enzyme with a Soret peak at 411 nm, which is different from that of native HRP (λ_{max} 402 nm). This result is consistent with the electronic absorption of the cyanoheme obtained from the HPLC diode array detector (Figure 2, inset). The cyanoheme-reconstituted enzyme had no catalytic activity for guaiacol oxidation (Table 1, experiment H) although more than 95% of the activity could be restored when native heme was used for reconstitution (Table 1, experiment G).

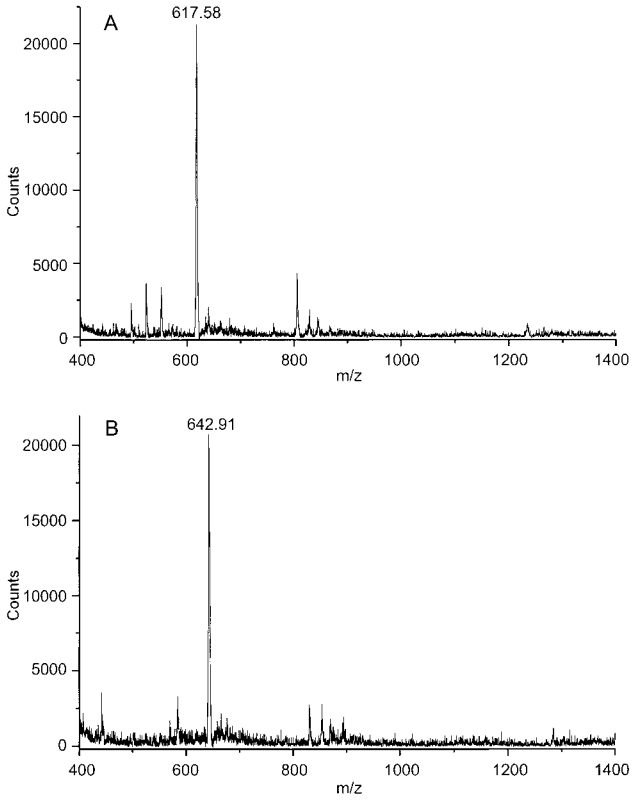

FIGURE 4: MALDI mass spectra of (A) native heme and (B) cyanoheme. The detailed conditions of HRP inhibition and heme isolation are described under Experimental Procedures and Results. The fractions eluted from the HPLC at retention times of 6.2 and 4.6 min were collected, lyophilized, and subjected to analysis by MALDI/MS as described under Experimental Procedures.

Structure of the Cyano-Derived Heme Group Isolated from Cyanide-Inactivated HRP. To identify the structure of the cyano-derived prosthetic heme group, the isolated hemes collected from HPLC (Figure 2) were subjected to MALDI/MS analysis. The mass spectrum of the species with a RT = 6.2 min contains a parent protonated molecule, $(M + H)^+$, of *m*/*z* 617.6 (Figure 4A), corresponding to an iron protoporphyrin IX (calculated molecular weight = 616.5). The mass spectrum of the species (RT = 4.6 min) expected to be a cyanoheme adduct contains an ion of *m*/*z* 642.9 (Figure 4B) that corresponds to the acquisition of one cyano group with the loss of one proton, suggesting that cyanyl radical was covalently incorporated into the iron protoporphyrin IX of HRP. Several other very minor adducts isolated by HPLC were also analyzed by MALDI/MS (data not shown): (1) RT = 4.1 min (Figure 2, peak c) and $(M + H)^+ = 658$, a molecular ion corresponding to the cyano-plus-one hydroxy adduct of heme; (2) RT = 5.3 min (Figure 2, peak d) and $(M + H)^+ = 633$, corresponding to a hydroxy adduct of heme; and (3) RT = 5.3 min (Figure 2, peak d) and $(M + H)^+ = 675$, corresponding to the cyano-plus-two hydroxy adduct of heme.

The 1D proton NMR spectra of the bipyridyl ferrous cyanoheme complex (Figure 5, Table 2) are consistent with the formation of a heme derivative with a cyano substitution at one of the *meso* positions. This is particularly apparent from the downfield spectral region showing only three *meso* proton resonances (Figure 5). It is obvious that one *meso* proton was lost and replaced by the cyano group, thus

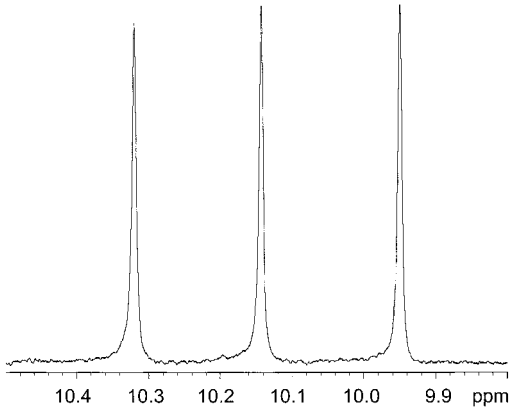

FIGURE 5: Pertinent region (three *meso*-protons) of the ^{1}H NMR (500 MHz) spectrum of the bipyridyl ferrous *meso*-cyanoprotoporphyrin IX isolated from cyanide-inactivated HRP. The NMR sample was prepared by dissolving the cyanoheme (ca. 2 mg) in 0.5 mL of pyridine-d_5. The proton NMR spectrum was acquired on a Varian UnityPlus 500 spectrometer operating at 499.875 MHz. The proton sweep width was 8000 Hz, and 30 722 total points were acquired for each scan. Sixty-four scans were signal-averaged, with a 90° pulse width of 6.3 μs and a 2-s relaxation delay between scans, for a total recycle time of 3.9 s. The time domain data were multiplied by an exponential window function with a line-broadening factor of 1 Hz prior to Fourier transformation.

unambiguously confirming the single heme-derived product as being a *meso*-cyanoheme. Comparison with the published spectral data on the native heme (Table 2) supports the interpretation that the substitution is at the *meso* position. The absence of scalar coupling interactions of the *meso* protons makes further assignment of the *meso* substitution position difficult. In a previous study of an azido heme derivative (*16*), through-space NOE interactions between the propionate methylene protons and the γ-*meso* proton were used to assign this *meso* position. In particular, we see a similar pattern of *meso* proton shifts, and the two internal vinyl protons of the *meso*-cyanoheme exhibit very little shift difference (0.09 ppm), similar to the corresponding protons in the *meso*-azidoheme (0.06 ppm). It would be anticipated that the shifts of the two internal vinyl protons should differ significantly if either of them is vicinal to the cyano group. Thus, it is unlikely that the cyanide is located at the α or β *meso* position. This conclusion is also consistent with the greater accessibility of the δ position to attack by the cyanyl radical (*17*).

The above data for δ-*meso*-cyanoheme isolated from the cyanide-inactivated HRP provide strong evidence that heme modification of HRP by cyanyl radical is, in part, involved in the mechanism of inhibition. We did not detect a significant protein-centered radical(s) in the reaction mixture of HRP/H_2O_2/KCN on the basis of the spin-trapping studies. As reported in the previous study (*5*), CcO can provide an alternative model system to study the interaction between cyanyl radical and hemoproteins.

Irreversible Inhibition of CcO by Potassium Cyanide. The cyanide radical can be detected as the DMPO/•CN adduct in the incubation of CcO and KCN with or without addition of H_2O_2 (*5*). In the absence of H_2O_2, the formation of cyanyl radical by CcO is time-dependent as reported previously (*5*). Figure 6A is the ESR spectrum of a reaction mixture containing 0.2 mM CcO, 10 mM KCN, and 100 mM DMPO recorded after roughly 3 min reaction time. The spectrum

Table 2: Comparison of Chemical Shift Values (in ppm) for Proton Signals in the $SnCl_2$-Reduced Dipyridyl Complexes of Native Heme and *meso*-Cyanohemes

proton	heme (*16*)	*meso*-cyanoheme[a] (experimental)
meso	10.283 (γ)	10.320
	10.236	10.143
	10.069	9.950
	9.906 (δ)	
methyls	3.623	3.922
	3.611	3.833
	3.468	3.480
	3.445	3.358
$-CH_2CH_2COOH$	4.467	4.518 (t, J = 7.5 Hz)
	4.461	4.457 (t, J = 7.5 Hz)
$-CH_2CH_2COOH$	3.504	3.846 (t, J = 7.0 Hz)
	3.484	3.467 (t, J = 7.0 Hz)
$-CH=CH_2$	8.510	8.312 (dd, J = 17.5, 11.5 Hz)
	8.451	8.226 (dd, J = 17.5, 11.5 Hz)
$-CH=CH_2$ (*cis*)	6.299	6.219 (dd, J = 16.5 Hz)
	6.269	6.186 (dd, J = 16.5 Hz)
$-CH=CH_2$ (*trans*)	5.960	6.062 (dd, J = 12.0 Hz)
	5.947	5.936 (dd, J = 12.0 Hz)

[a] A reaction mixture containing HRP (50 μM), potassium cyanide (5 mM), DTPA (1 mM), and H_2O_2 (10 mM) in 100 mL of 50 mM phosphate buffer (pH 7.4) was incubated at room temperature for 1 h. The excess peroxide was destroyed by adding 25 μL of catalase (10 mg/mL). Five minutes later, the enzyme was reduced to the ferric state by adding 200 μL of sodium ascorbate (200 mM). Glacial acetic acid (45 mL) was then added, and the heme was extracted with two 100 mL portions of diethyl ether. The combined ether layers were washed with water three times, dried over anhydrous sodium sulfate, and evaporated to dryness with a rotary evaporator. The cyanoheme was isolated by preparative HPLC on a 10 × 250 mm Altex Ultrasphere-ODS preparative column[b] at a flow rate of 2 mL/min. The eluate was monitored at 402 nm. The fraction containing cyano-derived heme with a retention time of 11.5 min was collected and converted to the chloroiron(III) form by partitioning between diethyl ether and 0.1 N DCl in NaCl-saturated D_2O. The chloroiron(III) derivative was dissolved in pyridine-d_5, reduced by a granule of $SnCl_2$, and then measured by ^{1}H NMR spectroscopy. The chemical shifts of the peaks were determined with reference to that of pyridine at 8.7 ppm. [b] The native heme and the cyano-derived heme eluted from this preparative column have retention times of 14.5 and 11.5 min, respectively.

was simulated as a combination of three species: DMPO/•CN (hyperfine coupling constants a^N= 15.43 and a_β^H = 18.90 G), DMPO/•OH (a^N = 15.0 and a_β^H = 14.8 G), and DMPO/•ScysCcO protein-derived thiyl radical (a^N= 14.68, a_β^H = 15.74 G, and line width = 3.12 G). The relative contributions of all three species are 0.05 for DMPO/•CN, 0.06 for DMPO/•OH, and 0.89 for DMPO/•ScysCcO. The formation of DMPO/•ScysCcO was prevented by pretreatment of CcO with *N*-ethylmaleimide (Figure 6C). The relative concentration of DMPO/•ScysCcO to DMPO/•CN was observed to be influenced by both the incubation time (Figure 6B) and the DMPO concentration (Figure 6D). As the incubation time was prolonged, or as the DMPO concentration was increased, the relative contribution of protein-derived thiyl radical was decreased, indicating that DMPO trapped •CN as the primary radical. The results indicated that the •CN was the primary radical, and the protein-derived thiyl radical was presumably formed from the reaction of cysteine residues of CcO with the highly reactive •CN.

To investigate whether the generated •CN would contribute to the inhibition of CcO, we dialyzed the reaction mixture overnight against 50 mM phosphate buffer, pH 7.4, containing 1% sodium cholate. The enzymatic activity of the dialysate was analyzed by cytochrome *c* oxidation and

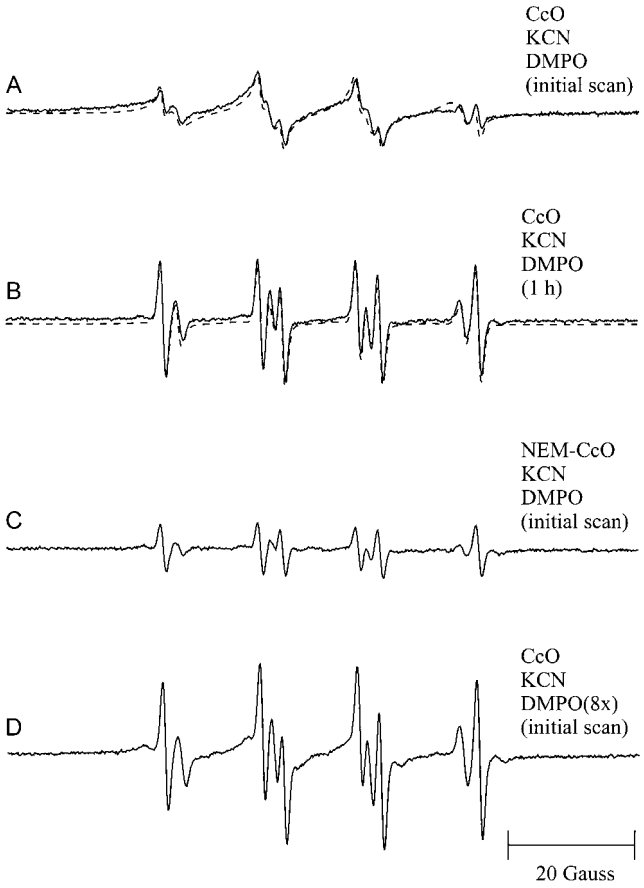

FIGURE 6: Effect of thiol-blocking reagent (*N*-ethylmaleimide) and high concentration of spin trap (DMPO) on the ESR spectrum from the reaction of purified cytochrome *c* oxidase and KCN. (A) The system contained CcO (0.2 mM), KCN (10 mM), and DMPO (100 mM) in 50 mM phosphate buffer, pH 7.4, containing 1 mM DTPA. The spectrum was recorded immediately after the reaction was initiated at room temperature. The spectrum produced by computer simulation (- - -) is superimposed upon the experimental spectrum (—). (B) Same incubation as in panel A, but the spectrum was recorded after 1 h of incubation. The spectrum produced by computer simulation (- - -) is superimposed upon the experimental spectrum (—). (C) Same incubation as in panel A, but the CcO was subjected to *N*-ethylmaleimide (NEM) pretreatment. (D) Same incubation as in panel A, but the concentration of DMPO was increased to 800 mM.

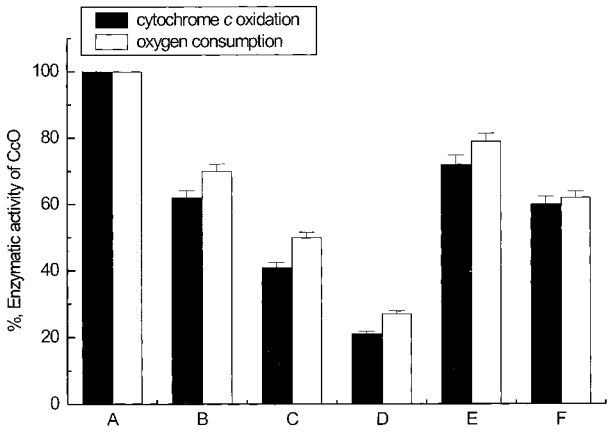

FIGURE 7: Effect of KCN and H_2O_2 on the enzymatic activity of purified cytochrome *c* oxidase. The reaction mixture containing CcO (0.2 mM), KCN, and H_2O_2 in 100 μL of 50 mM phosphate buffer (pH 7.4) containing 1 mM DTPA was incubated at room temperature. The reaction mixture was immediately dialyzed against the same buffer containing 1% sodium cholate for 8 h with one change of buffer. Cytochrome *c* oxidation activity (black bars) and oxygen consumption (white bars) were determined for aliquots of the dialysate. The activity was calculated on the basis of the CcO protein concentration determined by the Lowry assay with bovine serum albumin as the standard (*18*). (A) Intact CcO; (B) reaction mixture contained CcO and 50 equiv of KCN; (C) same mixture as B, but 5 equiv of H_2O_2 was included in the system; (D) same mixture as B, but the reaction proceeded for 1 h prior to dialysis; (E) same mixture as B, but KCN was decreased to 5 equiv; (F) same mixture as *E*, but 5 equiv of H_2O_2 was included in the system.

oxygen consumption (*18*). As indicated in Figure 7B, incubation of CcO with 50 equiv of KCN resulted in 37% inhibition of enzyme activity (cytchrome *c* oxidation). When H_2O_2 was included in the system, 58% inhibition was obtained (Figure 7C). Because H_2O_2 does not inhibit the activity of CcO (*14*), this additional inhibition must be due to the formation of additional cyanyl radicals. However, 80% inhibition was observed when the incubation time was prolonged up to 1 h (Figure 7D), indicating that at least 43% of inhibition came from cyanyl radical. Reduction of the amount of KCN to 5 equiv CcO decreased the inhibition to 28% (without H_2O_2, Figure 7E) and 40% (with H_2O_2, Figure 7F), presumably because less cyanyl radical was produced.

The heme *a* was isolated from the cyanide-inactivated CcO (with H_2O_2 and without H_2O_2 included in the system) by cold HCl/acetone/ether extraction and subjected to MALDI/MS analysis. The mass spectrum of this *a*-type iron protoporphyrin IX (calculated molecular weight = 852.4) exhibits an $(M + H)^+$ ion of *m*/*z* 853.6 (data not shown), which is the same as that of native heme *a*, suggesting that the heme edge did not react with cyanyl radical, in contrast to HRP. The pyridine hemochromogen spectrum of heme *a* purified from the cyanide-inactivated CcO is identical to that isolated from native CcO (λ_{max} of the α band by dithionite reduction = 588 nm, data not shown).

In fact, we were able to show that the cyanyl radical is actually generated by the CcO, and it can potentially be incorporated into iron protoporphyrin IX. Incubation of CcO, KCN, and added heme at room temperature for 1 h resulted in a single heme derivative (RT = 4.6 min) as detected by HPLC in addition to native heme (RT = 6.2 min) and the heme *a* (RT= 21.0 min) (data not shown). The retention time of this heme derivative is the same as that of *meso*-cyanoheme obtained from the HRP/H_2O_2/KCN system (Figure 2). The *m*/*z* value of the $(M + H)^+$ obtained from the MALDI/MS is the same as that of the *meso*-cyanoheme identified previously.

DISCUSSION

In this investigation, our results clearly demonstrate that the catalytic turnover of cyanide by HRP in the presence of H_2O_2 is essential for the irreversible inhibition of enzymatic activity by cyanide. The cyanyl radical was catalytically generated and detected by the spin-trapping technique. The cyanyl radical covalently added to the prosthetic group of HRP to yield a δ-*meso*-cyanoheme adduct. This characteristic radical chemistry supports the spin-trapping results and makes the artificial formation of DMPO/$^{\bullet}$CN unlikely (*9*, *10*). The only evidence for the latter proposal is the calculated high oxidation potential of cyanide. If formed, one logical

Scheme 1: Proposed Mechanism for Incorporation of the Cyano Group into the *δ-meso*-carbon of the Prosthetic Heme Group of HRP[a]

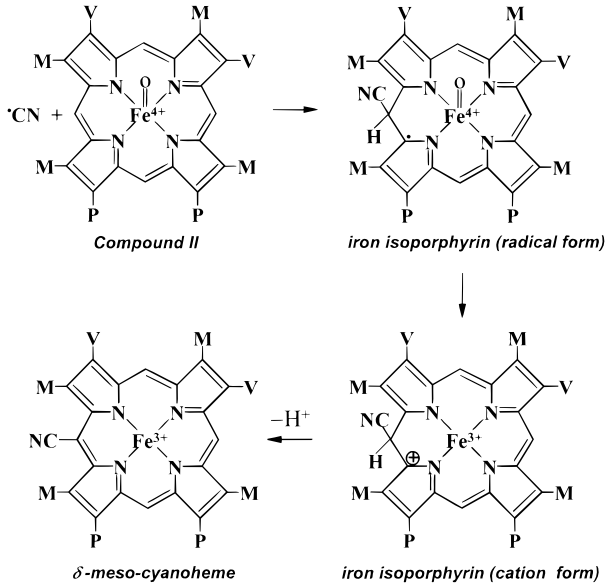

[a] Abbreviations: M, methyl; P, propionic acid; V, vinyl.

fate for cyanyl radical is to react with the enzyme itself. This reaction could occur with either the protein matrix or its prosthetic group. The detection of *meso*-substituted heme obtained from cyanide-inactivated HRP provides strong evidence for the latter case. We cannot determine whether the cyanyl radical also attacks the globin of HRP, although no protein-derived radical adduct has been detected (*2*, *3*). The addition of cyanyl radical to the heme is regiospecific for the *δ-meso* position (Figure 5 and Table 2) for steric reasons as supported by the X-ray crystallographic data of HRP (*17*). This regiospecific modification was also observed in the study of peroxidase induced by azide inhibition (*16*).

As discussed in the previous study (*5*), both HRP compounds I and II were proposed to produce the cyanyl radical under catalytic turnover conditions:

Reaction 1

$$\text{HRP} + \text{H}_2\text{O}_2 \rightarrow \text{HRP compound I} + \text{H}_2\text{O}$$

Reaction 2

$$\text{HRP compound I} + \text{CN}^- \rightarrow \text{HRP compound II} + {}^{\bullet}\text{CN}$$

The steady-state concentration of $^{\bullet}$CN is low due to its reactivity, and this drives the above reaction (reaction 2) toward completion. In a subsequent step, the cyanyl radical added across the heme edge of HRP compound II. That is, the cyanyl radical was incorporated into the *δ-meso* position by nucleophilic addition, which then yielded a *meso*-cyanoheme by loss of a *meso*-proton (Scheme 1). Two isoporphyrin intermediates are suggested to participate in the proposed mechanism (Scheme 1). Presumably, these isoporphyrin intermediates are not stable and rapidly form product (*19*).

In the case of CcO, the catalytically generated cyanyl radical is formed independently of exogenous H_2O_2. In the presence of H_2O_2, the enzyme proceeds via typical peroxidase chemistry to oxidize the cyanide at a higher reaction rate than that of the as-isolated CcO/cyanide system (*5*). It is well-known that the affinity of cyanide as the sixth ligand of heme a_3 in CcO is relatively high and causes inhibition of the enzyme. The cyanyl radical generated under the turnover condition (with or without H_2O_2), however, also partially contributed to the inhibition of CcO (Figure 7). Unlike the results observed for cyanide-inactivated HRP, the heme *a* isolated from both CcO/KCN and CcO/KCN/H_2O_2 reaction mixtures did not exhibit any modification based on its MALDI mass spectral data or the pyridine hemochromagen absorption spectrum (data not shown). The possible formation of a cyano−iron σ complex can be eliminated on the basis of the MALDI/MS results.

Conceivable reasons for the different inhibition mechanisms of HRP and CcO by cyanyl radical can be attributed to differences in the structure and/or the environment of their active sites. The structure of CcO heme *a* contains a 1-formyl substituent and a 7-hydroxyl farnesylethyl group. The three-dimensional X-ray structure of CcO revealed that the heme *a* and heme a_3 are located 13 Å into the inner membrane of 48 Å thickness. Each heme is held by its four transmembrane helices (of subunit I) arranged in a semicircular shape (*20*, *21*). Two channels observed in the crystal structure are of interest and give direct access to the active site of heme a_3. One of them is a possible O_2 channel, in that most amino acid residues lining the channel are aromatic or hydrophobic, and the other is a possible channel for protons and for releasing water. Two key amino acid residues, including a lysine (K319) and a modified tyrosine (Y244), are critical for this channel. It is logical to propose that the *meso*-proton of the heme a_3 is protected by the protein residues and the hydroxyl farnesylethyl group and is, thus, inaccessible to the cyanyl radical.

Our spin-trapping study indicated that an immobilized sulfur-centered radical was detected in the CcO/KCN reaction mixture (Figure 6A,C). Increasing the DMPO concentration decreased the relative amount of the CcO-derived thiyl radical detected, suggesting that the protein-derived thiyl radical was derived by $^{\bullet}$CN attack and formed as a secondary radical (Figure 6D). Nevertheless, evidence has shown that chemical modification of CcO by *N*-ethylmaleimide or selective generation of thiyl radical on CcO by Ce^{4+} did not cause significant inhibition of enzyme activity (*14*). It is likely that the oxidative damage by $^{\bullet}$CN attack can be thermodynamically transferred from thiyl radical intermediates to carbon-centered radicals as reported by Prutz et al. (*22*). Currently, it is not clear what intramolecular pathway is involved in producing the thiyl radical on CcO. Interestingly, the crystallographic data show that tyrosine 244 is cross-linked to one of the Cu_B ligands, histidine 240, and is close to the heme a_3 (*23*). It has been proposed that this modified tyrosine is important for enzyme turnover and proton pumping (*24*−*26*). We speculate that it is also possible to form a tyrosyl radical in CcO and then establish a radical equilibrium with cysteine residue(s) as seen in the case of the inactivation of xanthine oxidase by oxidative radical attack (*27*). Based on the previous study (*5*), the discussion above, and the results from this investigation, we propose the following mechanism to explain the inhibition of CcO by $^{\bullet}$CN:

Reaction 3

$$\text{compound P} + CN^- \rightarrow \text{compound F} + {}^{\bullet}CN$$

Reaction 4

$$\text{compound F} + CN^- \rightarrow \text{CcO} + {}^{\bullet}CN$$

Reaction 5

$${}^{\bullet}CN + \text{TyrCcO} \rightarrow CN^- + {}^{\bullet}\text{OTyrCcO}$$

Reaction 6

$${}^{\bullet}\text{OTyrCcO} \leftrightarrow {}^{\bullet}\text{SCysCcO}$$

The cyanyl free radical is extremely reactive. Therefore, •CN-induced enzyme inhibition is probably the result of damage to the protein. In addition to the effect on the protein matrix, the •CN generated by CcO can also form cyanoheme adducts when purified iron protoporphyrin IX is included under the turnover condition (data not shown). The results here imply that the highly reactive •CN may migrate and cause damage on the prosthetic groups of other hemoproteins such as cytochrome *c* that are in proximity to CcO or may induce an oxidative stress event such as lipid peroxidation.

ACKNOWLEDGMENT

We thank Drs. Robert E. London and Bennett van Houten for critical review of the manuscript. We also gratefully acknowledge the help of Dr. Robert E. London for discussing the NMR data and Dr. Eugene F. DeRose for obtaining the NMR spectrum of *meso*-cyanoheme, and the assistance of Ms. Mary Mason for polishing the English of this manuscript.

REFERENCES

1. Solomonson, L. P. (1981) in *Cyanide in Biology* (Vennesland, B., Conn, E. E., Knowles, C. J., Westley, J., and Wissing, I., Eds.), pp 11−28, Academic Press, New York.
2. Moreno, S. N. J., Stolze, K., Janzen, E. G., and Mason, R. P. (1988) *Arch. Biochem. Biophys. 265*, 267−271.
3. Stolze, K., Moreno, S. N. J., and Mason, R. P. (1989) *J. Inorg. Biochem. 37*, 45−53.
4. Palmer, G. (1993) *J. Bioenerg. Biomembr. 25*, 145−151.
5. Chen, Y.-R., Sturgeon, B. E., Gunther, M. R., and Mason, R. P. (1999) *J. Biol. Chem. 274*, 24611−24616.
6. Fabian, M., and Palmer, G. (1995) *Biochemistry 34*, 1534−1540.
7. Konstantinov, A. A., Vygodina, T., Capitanio, N., and Papa, S. (1998) *Biochim. Biophys. Acta 1363*, 11−23.
8. Zaslavsky, D., and Gennis, R. B. (1998) *Biochemistry 37*, 3062−3067.
9. Eberson, L. (1998) *Adv. Phys. Org. Chem. 31*, 91−141.
10. Eberson, L., and Persson, O. (1998) *Acta Chem. Scand. 52*, 608−621.
11. Forrester, A. R., and Hepburn, S. P. (1971) *J. Chem. Soc. C*, 701−703.
12. Pearson, R. G. (1986) *J. Am. Chem. Soc. 108*, 6109−6114.
13. Yu, C.-A., Yu, L., and King, T. E. (1975) *J. Biol. Chem. 250*, 1383−1392.
14. Chen, Y.-R., Gunther, M. R., and Mason, R. P. (1999) *J. Biol. Chem. 274*, 3308−3314.
15. Duling, D. R. (1994) *J. Magn. Reson. Ser. B 104*, 105−110.
16. Ortiz de Montellano, P. R., David, S. K., Ator, M. A., and Tew, D. (1988) *Biochemistry 27*, 5470−5476.
17. Gajhede, M., Schuller, D. J., Henriksen, A., Smith, A. T., and Poulos, T. L. (1997) *Nat. Struct. Biol. 4*, 1032−1038.
18. Lowry, O. H., Rosebrough, N. J., Farr, A. L., and Randall, R. J. (1951) *J. Biol. Chem. 193*, 265−275.
19. Ator, M. A., David, S. K., and Ortiz de Montellano, P. R. (1989) *J. Biol. Chem. 264*, 9250−9257.
20. Tsukihara, T., Aoyama, H., Yamashita, E., Tomizaki, T., Yamaguchi, H., Shinzawa-Itoh, K., Nakashima, R., Yaono, R., and Yoshikawa, S. (1995) *Science 269*, 1069−1074.
21. Tsukihara, T., Aoyama, H., Yamashita, E., Tomizaki, T., Yamaguchi, H., Shinzawa-Itoh, K., Nakashima, R., Yaono, R., and Yoshikawa, S. (1996) *Science 272*, 1136−1144.
22. Prütz, W. A., Butler, J., Land, E. J., and Swallow, A. J. (1986) *Free Radical Res. Commun. 2*, 69−75.
23. Yoshikawa, S., Shinzawa-Itoh, K., Nakashima, R., Yaona, R., Yamashita, E., Inoue, N., Yao, M., Fei, M. J., Libeu, C. P., Mizushima, T., Yamaguchi, H., Tomizaki, T., and Tsukihara, T. (1998) *Science 280*, 1723−1729.
24. Proshlyakov, D. A., Pressler, M. A., and Babcock, G. T. (1998) *Proc. Natl. Acad. Sci. U.S.A. 95*, 8020−8025.
25. Gennis, R. B. (1998) *Biochim. Biophys. Acta 1365*, 241−248.
26. Thomas, J. W., Calhoun, M. W., Lemieux, L. J., Puustinen, A., Wikström, M., Alben, J. O., and Gennis, R. B. (1994) *Biochemistry 33*, 13013−13021.
27. Anderson, R. F., Hille, R., and Patel, K. B. (1995) *Int. J. Radiat. Biol. 68*, 535−541.

BI992652+